Journal of Crystal Growth 336 (2011) 72–76

Contents lists available at SciVerse ScienceDirect

Journal of Crystal Growth

journal homepage: www.elsevier.com/locate/jcrysgro

Fabrication of high density, adherent films of five-fold symmetric diamond crystals by hot filament chemical vapour deposition

Qiuping Wei [a,b,c], M.N.R. Ashfold [b], Z.M. Yu [a,*], Li Ma [c], D.F. Yin [a]

[a] School of Materials Science and Engineering, Central South University, Changsha 410083, PR China
[b] School of Chemistry, University of Bristol, Bristol BS8 1TS, United Kingdom
[c] State Key Laboratory of Powder Metallurgy, Central South University, Changsha 410083, PR China

ARTICLE INFO

Article history:
Received 9 January 2011
Received in revised form
1 August 2011
Accepted 6 September 2011
Communicated by J.B. Mullin
Available online 16 September 2011

Keywords:
A1. Adhesion
A1. Five-fold symmetric
A1. Fretting wear
A3. CVD
B1. Diamond

ABSTRACT

Five-fold symmetric diamond crystals (FSDCs) have been grown on a large variety of substrates by hot filament chemical vapour deposition (CVD) methods. High density, adherent films of FSDCs have been prepared on carbon steel with a thermal sprayed WC–Co interlayer, and their quality, adhesion and tribological behaviour were investigated. The diamond films show excellent adhesion under Rockwell indentation testing and when subjected to high-speed, high-load, long-time reciprocating dry sliding ball-on-flat wear tests against a Si_3N_4 counter-face in ambient air.

1. Introduction

Numerous five-fold symmetric structures have been reported since the discovery of metallic solids with icosahedral point group symmetry [1]. Many are associated with face-centred cubic systems, especially aluminium alloys (e.g., Al–Li–Cu, Al–Mn–Si, Al–Ni–Co, Al–Pd–Mn, Al–Cu–Fe, etc.), but other compositions are also known (e.g., Cd–Yb, Ti–Zr–Ni, Zn–Mg–Ho, Zn–Mg–Sc, In–Ag–Yb and Pd–U–Si) [2]. Five-fold symmetric (especially icosahedral) structures exhibit many notable properties including high hardness and elastic modulus, low friction and remarkable electronic properties (e.g., very anisotropic electronic transport) [3,4], and consequently attract much publicity [4–9]—not least in the context of carbon structures [10–13]. Growth of five-fold symmetric diamond crystals (FSDCs) by chemical vapour deposition (CVD) methods was first reported by Matsumoto and Matsui [14]. The intervening period has witnessed considerable interest in the formation mechanism, atomic structure and defects of FSDC and icosahedral carbon clusters [10–12,14–20]. FSDC formation has been variously explained by invoking three stacking errors during growth on different (111) surfaces [16], arising as a result of the interaction between two $\Sigma = 3$ {111} twin boundaries and an intrinsic stacking fault [19,20] or in terms of growth on a molecular nucleus [14]. Here we explore the influence of hot filament (HF) assisted CVD conditions on FSDC growth on a wide range of substrates and demonstrate the production of dense, adherent films with high FSDC content.

2. Experimental details

FSDCs were deposited on a range of substrates from an activated methane/hydrogen gas mixtures in a HFCVD reactor, details of which have been reported previously [21,22]. Si(100), Si(111), tungsten, titanium, molybdenum, beryllium oxide, AISI 1085 carbon steel, WC–Co cemented carbide and AISI 1085 carbon steel pre-coated with a high velocity oxy-fuel (HVOF) sprayed WC–Co layer were investigated as substrates. The filament temperature (T_f) was measured by an optical pyrometry. K-type thermocouples attached to the substrate surface enabled measurement of the substrate temperature (T_s), which was controlled by T_f and the filament to substrate distance (d_f), i.e., there was no active cooling of the substrate during the HFCVD process. The gas activation induced by the HF at T_f, the gas chemistry and the precursor concentrations at the growth interface and T_s are thus inevitably all strongly coupled. The base pressure ($< 1 \times 10^{-6}$ Torr) was maintained by a turbomolecular

---

* Corresponding author at: School of Materials Science and Engineering, Central South University, Changsha 410083, PR China. Tel.: +86 731 88830335; fax: +86 731 88876692.
E-mail addresses: qiupwei@csu.edu.cn (Q. Wei), zhiming@mail.csu.edu.cn (Z.M. Yu).

0022-0248/$ - see front matter Crown Copyright © 2011 Published by Elsevier B.V. All rights reserved.
doi:10.1016/j.jcrysgro.2011.09.017

Table 1
Experimental parameters used for diamond film deposition on specimens I and II.

	Specimen type	
	I	II
Substrate	WC–13 wt% Co	AISI 1085 carbon steel with HVOF sprayed WC–Co interlayer
Hot filament power (W)	390	400
Hot filament current (A)	19.8	16.5
Substrate temperature (°C)	740	760
CH_4/H_2 (vol.%)	3	3
Deposition pressure (kPa)	2.67	3
Total gas flow rate (sccm)	20	50
Deposition time (min)	90	300

pump, and the deposition pressure (p) monitored and controlled using a manometer. All of the substrates investigated support FSDC growth under appropriate CVD conditions. Deposition parameters were varied in the range: filament power, $P=$ 350–570 W; filament current, $I=16$–21 A; $T_f=1900$–2300 °C; $p=5$–60 Torr; $T_s=500$–1000 °C; methane mole fraction, $C_m=$ 1–6% in hydrogen; total flow rate, $F_g=20$–100 standard cm^3 per min (sccm); deposition time, $t=20$–3000 mins. Table 1 shows the CVD parameters used for two sets of specimens (henceforth termed as specimens I and II), which were typically held constant for each specimen and deposition. For specimen I, diamond films were grown on a WC–13 wt% Co sample with the dimension of $6\times6\times3$ mm^3. This was first etched by ultrasonicating in Murakami's reagent [23] for 20 min to enhance the surface roughness. Surface Co was then removed by etching in an acidic solution of the hydrogen peroxide. The substrate was then abraded ultrasonically in a suspension of nanodiamond powder in acetone for 20 min and finally cleaned ultrasonically in acetone and ethanol prior to diamond growth by CVD. For specimen II, diamond films were grown on an AISI 1085 carbon steel plate ($10\times10\times5$ mm^3) with a Co-containing tungsten carbide (WC–Co) interlayer deposited by HVOF. The WC–Co blends typically comprised 85–90% WC and 10–15% Co powder (powder size ~2–5 μm), and the spraying parameters were $F(O_2)=57$ m^3/h; spray distance 30 cm and fuel rate 23 dm^3/h. The as-deposited WC–Co interlayer was polished (diamond polishing agent) to reduce its surface roughness. These specimens were then etched using a two-step pre-treatment comprising: (i) ultrasonic etching using Murakami's reagent for 3 min; (ii) removal of surface Co by etching in an acidic solution of hydrogen peroxide for 2 min, then abraded and cleaned as in the case of the WC–13 wt% Co substrate prior to CVD growth.

Specimens were characterized by a variety of techniques, including field emission scanning electron microscopy (SEM, FEI, Sirion200 Field-emission SEM), X-ray diffraction (XRD: Dmax-2500VBX using CuK_α radiation at a wavelength of 0.154 nm), energy dispersive X-ray analysis (EDX: EDAX model) and Raman spectroscopy (LabRAM HR800). Raman spectra were measured with an argon ion laser operating at 488 nm with an output power of 100 mW. The cross-sections of the specimens after indentation testing were obtained by polishing them with diamond abrasive paste and subsequently ultrasonically etching in Murakami solution for 1 min. Adhesion was investigated further using a Rockwell hardness tester with a Brale diamond indenter (angle $=120^\circ$, radius $=0.2$ mm) at loads of 600, 1000 and 1500 N. Friction and wear tests were conducted using a ball-on-disc tribometer (High Load, Heavy Duty Tribometer, UMT-3, CETR, USA), in an open air, at ambient temperature and at a relative humidity of (65 ± 5)%. A 9.5 mm diameter silicon nitride ball with surface finish better than 0.1 μm was loaded as the counter-face to a diamond coated flat steel substrate (specimen II) mounted on a horizontal translation table. A load (F_z) of 50 N was applied to the Si_3N_4 ball, while the specimen was subjected to a reciprocating displacement of ~4 mm with a sliding velocity, $V=1000$ rpm (~17 Hz). The coefficient of friction (COF) was obtained by measuring the tangential force (F_f) exerted on the ball during sliding.

3. Results and discussion

Fig. 1 shows SEM images of isolated FSDCs (the precursors to a continuous polycrystalline diamond film) grown on a selection of these substrates. High energy ultrasonic treatment (in any of a range of different solvents like water, acetone and ethanol) offers a means of removing such FDSCs from their original substrate, forming a suspension in solution and transferring the FSDCs to, e.g., a holey carbon grid for TEM analysis. It is trivial to achieve a low nucleation density on smooth single crystal silicon but, as Fig. 1(a) shows, SEM imaging of small diamond crystals deposited on such surface is challenging. Fig. 1(b) and (c) demonstrates growth of isolated FSDCs on AISI 1085 carbon steel substrates; these FSDCs show evidence of etching at the twin-plane boundary. The high solubility of carbon in the fcc phase of iron in this case ensures the long nucleation times [24] and low nucleation densities needed for observation of isolated FSDCs. Tungsten is less prone to carbide formation than Ti, Mo (or Fe) under typical diamond growth conditions, and was thus the substrate of choice (99.9 wt%, size: $6\times6\times3$ mm^3) for most of the present studies. It proved advantageous to pre-coat these W substrates with a thin tungsten film (purity 99.99 wt%) by *in situ* magnetron sputtering prior to diamond CVD. The abundant boundaries and nanoscale defects in the sputtered coating leads to higher surface activity, increased carbon solubility, reduced nucleation densities and consequent formation of high quality isolated FSDCs—as illustrated in Fig. 1(d)–(l).

Successful FSDC formation is sensitive to the choice of substrate and to the CVD process conditions. The pre-mixed source gas for all specimens discussed here entered the reactor through a 4 mm i.d. stainless steel pipe that penetrates the reactor wall and terminates 3 cm from the single HF. With this arrangement, FSDC growth was discerned throughout the following parameter space: $P=380$–550 W; $I=16.4$–20.8 A; $p=2.6$–3.9 kPa; $T_s=700$–850 °C; $C_m=1$–4% and $F_g=20$–100 sccm. The conditions required to grow films with high FSDC content are far more stringent. Fig. 1(k) and (l) shows SEM images of diamond crystallites grown on W-sputter coated W substrates at $P=450$ W; $I=20.8$ A; $p=3.0$ kPa; $T_s=730$ °C; $F_g=50$ sccm and $C_m=3$% for $t=15$ mins, then with $C_m=1$% for a further $t=240$ min; the FSDC content in these samples is ~50%.

We have recently investigated a range of pre-treatment methods for diamond films deposited on sintered WC–Co substrates with different cobalt contents [23,25]. Two-step pretreatment is straightforward and relatively cheap, and shown to work well for WC–Co substrates [25]. The substrate used for the near-continuous film shown in Fig. 1(m)—specimen I—was a WC–13 wt% Co sample ($6\times6\times3$ mm^3) with two-step pretreatment. The relative FSDC content in this film is >30%.

Iron catalyzes graphite formation at diamond/steel interfaces during the CVD process [26,27] and the high solubility of carbon in the iron fcc phase results in prolonged diamond nucleation times [24,28]. Diamond and steel have very different coefficients of thermal expansion, which result in high stress within any diamond film deposited directly on steel[24]. For all these reasons, direct growth of high density, adherent diamond films

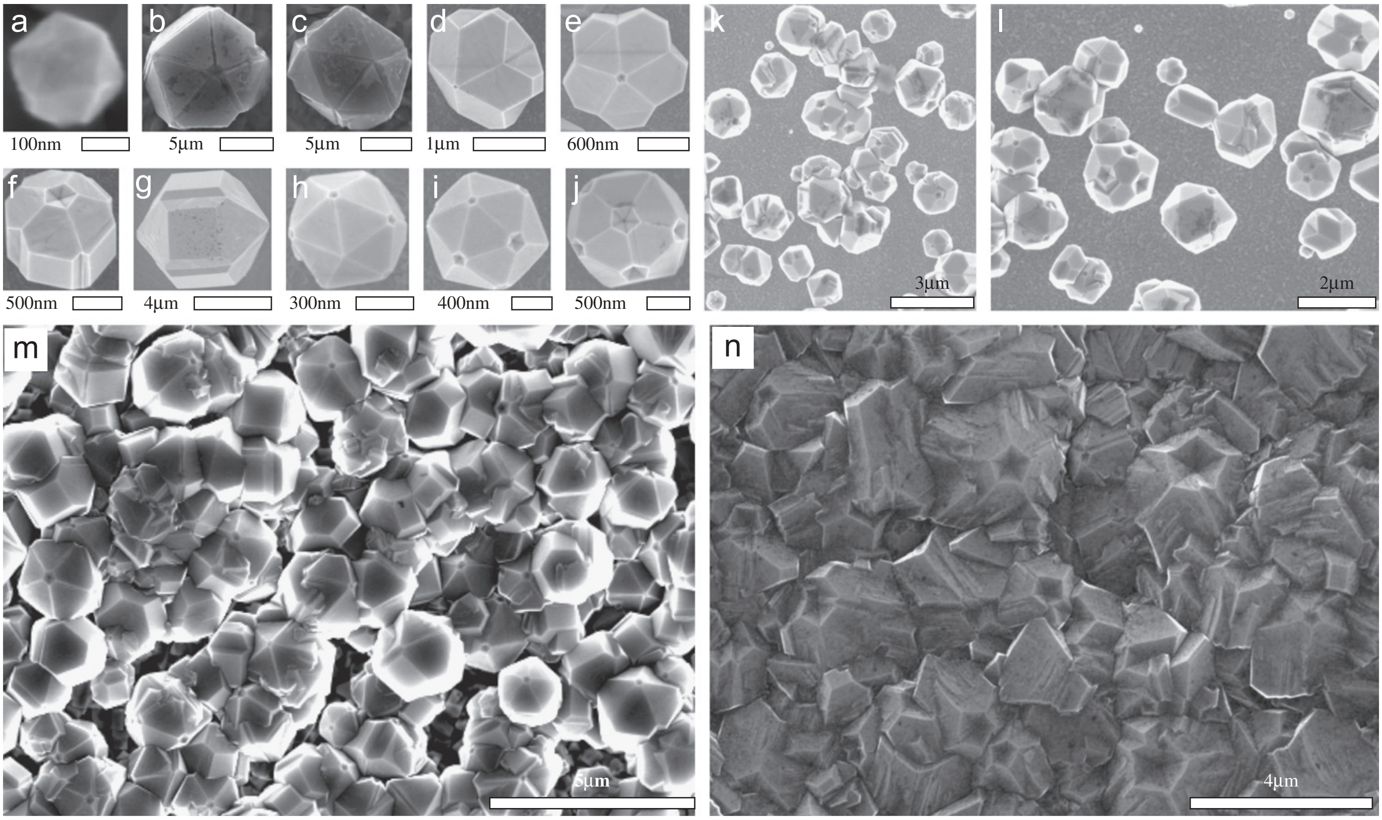

Fig. 1. SEM images of FSDCs grown on: (a) Si (100); (b, c) AISI 1085 carbon steel; (d–l) tungsten, over-coated with a sputtered tungsten film; (m) WC–13 wt%Co cemented carbide; (n) AISI 1085 carbon steel with a HVOF sprayed WC–Co coating.

on steel substrates is very difficult [29–31], and modification of the substrate surface, and/or the use of interlayers, is necessary in order to improve the quality and adhesion of any such diamond coating. We have recently reported HFCVD of adherent diamond films on steel substrates that had themselves been pre-coated with a thin WC–Co interlayer [32,33]. Successful diamond growth was achieved after pre-treating the WC–Co interlayer with a two-step etching process, which had the effect of depleting the Co content at the surface. Diamond growth was shown to be accompanied by some additional carburization of the pre-treated WC interlayer, which encourages film adhesion. The film shown in Fig. 1(n) was grown on an AISI 1085 carbon steel plate ($10\times10\times5$ mm^3) with a Co-containing tungsten carbide (WC–Co) interlayer deposited by HVOF—and is an example of specimen II. SEM image analysis suggests $>80\%$ FSDC content across the entire sample area.

We have previously reported diamond film growth in this same HFCVD reactor on WC–Co bar substrates, at a range of methane concentrations ($C_m=1$, 2 or 4%) and total gas pressures ($p=2$, 5 or 9 kPa) [34]. Each substrate was positioned to span a range of d_f values (6–24 mm), and thus substrate temperatures ($T_s=500$–900 °C) and incident gas phase chemistry and compositions. FSDCs were only identified in the narrow range $6<d_f<11$ mm and the FSDC content was $<10\%$ under all conditions, but these studies did suggest that FSDC formation is favored by low C_m and/or low p.

The present observations suggest that the gas chemistry and composition at the growing diamond surface must be important for FSDC growth. 2- and 3-D models of the gas chemistry accompanying HFCVD [35,36] highlight the importance of H_2 dissociation at the filament surface and the subsequent diffusion of H atoms throughout the reactor volume. H atoms drive the inter-conversion between C_1 (C_1H_y) and C_2 (C_2H_x) species—both via radical forming (so-called "H-shifting") abstraction reactions and, in the cooler regions, by a sequence of third-body stabilized H addition reactions that culminate in the conversion of C_2H_x species to members of the C_1H_y family [37]. The H atom concentration drops as a result of H abstraction and H addition reactions at the substrate. Growth under the present experimental conditions is expected to depend sensitively upon T_s and the H atom and CH_3 radical densities adjacent to the substrate surface.

Fig. 2(a) shows Raman spectra of the films deposited on specimens I and II. Both show obvious diamond peaks, centred at $\sim$1335.4 cm^{-1} (specimen I) and $\sim$1337.1 cm^{-1} (specimen II); the latter peak is broader and rides on a background signal associated with graphitic (sp^2-bonded) carbon. The ratio of the diamond intensity to that of the $\sim$1550 cm^{-1} feature characteristic of sp^2 carbon is larger for the film on specimen I, indicating that this is the higher quality diamond film. Both diamond peaks are somewhat blue-shifted relative to the peak position in stress-free diamond (1332.2 cm^{-1}), suggesting the presence of some compressive stress in the deposited films—possibly attributable to the mismatch in thermal expansion between the substrate and the diamond film [38].

X-ray diffraction spectra of CVD diamond films grown on specimens I and II are shown in Fig. 2(b). Peaks at 2θ diffraction angles of 44.0°, 75.4° and 91.4°—corresponding to, respectively, the (111), (220) and (311) reflections of the cubic diamond structure—are evident in both spectra, though the relative intensities of the WC features are much stronger in the XRD spectrum of the sample on the WC–Co substrate (specimen I). Note that the peak at $2\theta\sim75.4°$ matches closely with the diamond (220) peak at 75.302° and the WC (200) peak at 75.477°; the observed feature is considered to be a blend of these two reflections (see inset to Fig. 2(b)). Comparing the relative intensities of the various diffraction peaks with the ASTM (American Society for Testing and Materials) data provides some information about the texture of these diamond films. The large $I_{(111)}/I_{(220)}$ and $I_{(111)}/I_{(311)}$ ratios for specimen II, in particular, imply a preference for $\langle 111 \rangle$ textured growth—consistent with the SEM images of this sample.

The blue-shift of the diamond peak in the Raman spectra (Fig. 2(a)) was taken as evidence that the films were under compressive stress—implying that the films are adhered to the underlying substrate. The cross-section images of an FSDC-coated steel substrate (specimen II, Fig. 3(a) and (b)) show a continuous tri-layer structure, with a ~200 μm thick, WC–Co interlayer and a ~6 μm thick diamond coating. As Fig. 3(c) shows, even with a 1500 N load, we observe no flaking-off of the diamond film around the indentation on specimen II—demonstrating the good adhesion of the diamond film. The inset in Fig. 3(c) shows part of one of the cracks evident in the main image recorded at higher magnification. AISI 1085 carbon steel will undergo plastic deformation under a load of 1500 N, but WC–Co is a hard, brittle material which cannot deform in synchrony with the steel substrate. Cracks generated by the WC–Co interlayer under a 1500 N load are thus inevitable. The cracking of the diamond film and the WC–Co interlayer is synchronous, however, demonstrating that the shearing forces in these two layers are not separated from the substrate [39].

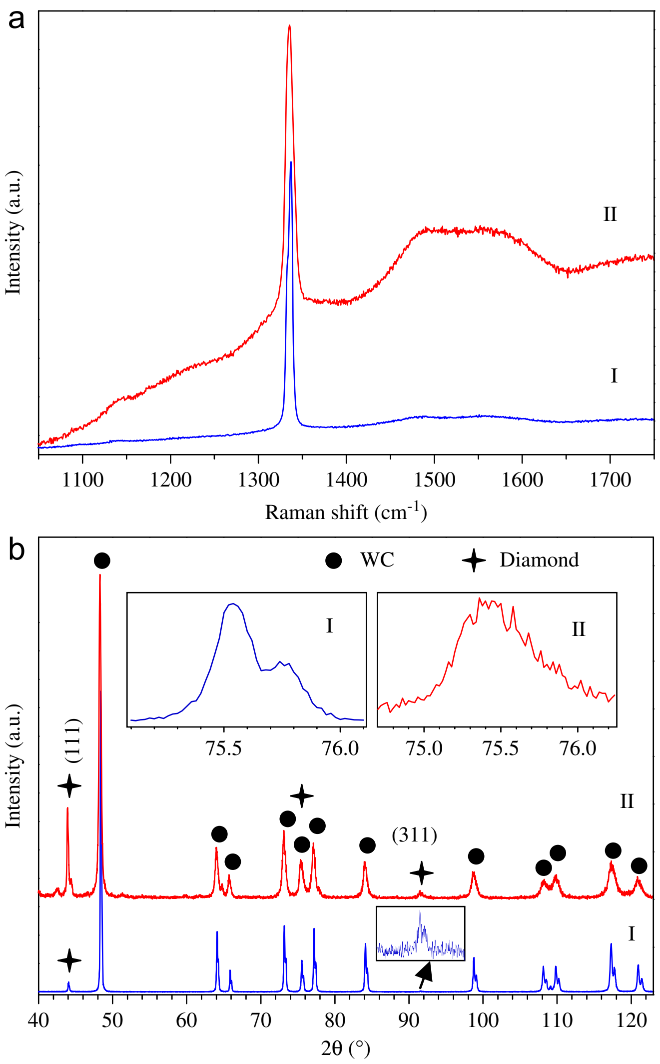

Fig. 2. (a) Raman and (b) XRD spectra of diamond films deposited on specimens I and II.

Fig. 3(d) shows an SEM image of the entire wear track, while Fig. 4 shows the time dependence of F_z, F_f and the COF. The measured COF for a Si_3N_4 ball sliding in air against a diamond film with high FSDC content on specimen II increases gradually with time but, even after 1,20,000 cycles, is still <0.045 and the diamond film has not worn through. We did not attempt any quantitative comparison of the wear resistance and friction response of these high FSDC content films with that of diamond films of similar thickness but little or no FSDC content, though wear resistance and friction measurements of films with low FSDC content have been reported previously [32,33]. There are so many factors that could affect the tribological properties in the diamond/WC–Co/steel system that it is very difficult to estimate whether or not a high FSDC content improves the tribological properties of these films; this could be a good topic for future research involving what is a relatively simple system.

4. Conclusions

We have established optimal HFCVD conditions for growing high quality FSDCs and diamond films with high FSDC content on a large variety of substrates, such as Si(100), Si(111), tungsten, titanium, molybdenum, beryllium oxide, AISI 1085 carbon steel, WC-Co cemented carbide and AISI 1085 carbon steel pre-coated with a high velocity oxy-fuel (HVOF) sprayed WC–Co layer. We have also established that high energy ultrasonic treatment, in several different solvents (e.g., water, acetone, ethanol, etc.), offers a means of removing FDSCs from their original substrate, forming suspensions of FDSCs in solution and transferring them to, e.g., a holey carbon grid. High density, adherent films with high FSDC content have been prepared on carbon steel with a thermal sprayed WC–Co interlayer. The diamond films show

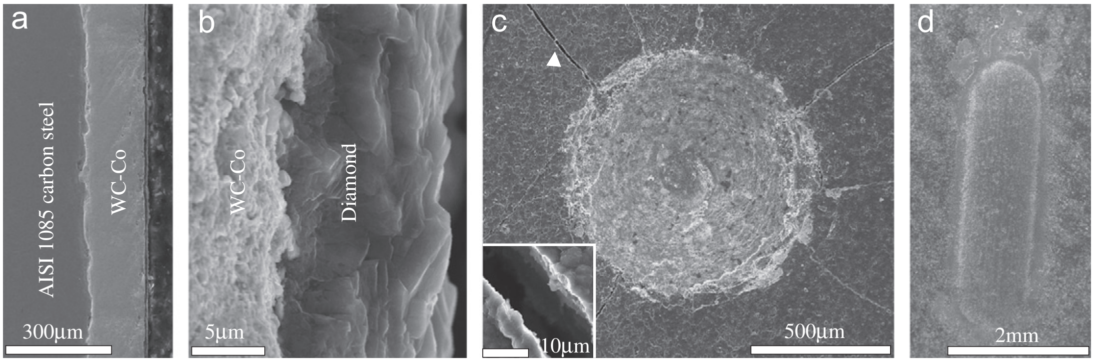

Fig. 3. SEM images of diamond films deposited on specimen II: (a) and (b), cross-sections through the film at different magnifications; (c) Rockwell indentation of this film, under a load of 1500 N (with a crack shown under higher magnification in the inset); (d) sliding wear track after reciprocating fretting testing of this film.

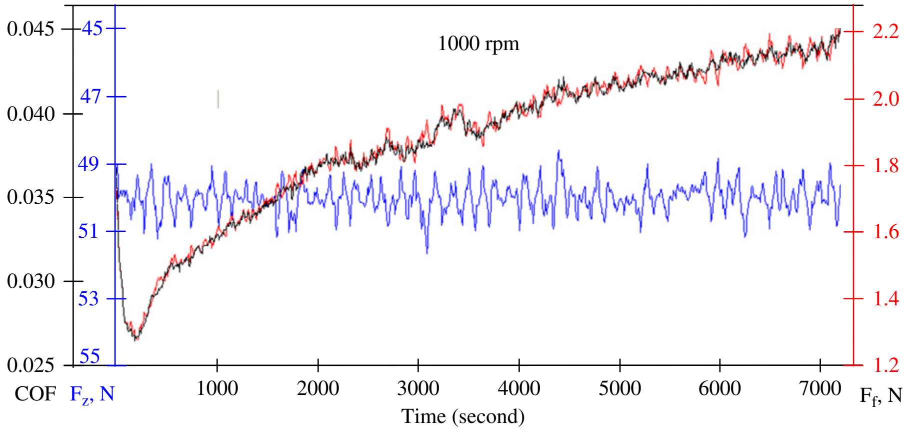

Fig. 4. Evolution of the COF of Si_3N_4 balls sliding against a diamond film on specimen II. The measurement involved reciprocating sliding tests, performed in ambient air, with a load of 50 N and no added lubricant.

excellent adhesion under Rockwell indentation testing and when subjected to high-speed, high-load, long-time reciprocating dry sliding ball-on-flat wear tests against a Si_3N_4 counter-face in ambient air.

Acknowledgements

We acknowledge the “China Scholarship Council”, the “State Key Laboratory of Powder Metallurgy”, the “Outstanding PhD Students Enabling Fund”, the “Innovation Foundation for Postgraduates of Hunan Province of China”, and the “Open Fund for Valuable Instruments of Central South University” for financial support.

References

[1] D. Shechtman, I. Blech, D. Gratias, J.W. Cahn, Physical Review Letters 53 (1984) 1951–1954.
[2] E. Maciá, Reports on Progress in Physics 69 (2006) 397–441.
[3] A. van Blaaderen, Nature 461 (2009) 892–893.
[4] M. Wakeda, Y. Shibutani, Acta Materialia 58 (2010) 3963–3969.
[5] Y. Gao, N. Shao, Y. Pei, X.C. Zeng, Nano Letters 10 (2010) 1055–1062.
[6] M. Burrello, H. Xu, G. Mussardo, X. Wan, Physical Review Letters 104 (2010) 160502.
[7] Y.T. Shen, T.H. Kim, A.K. Gangopadhyay, K.F. Kelton, Physical Review Letters 102 (2009) 057801.
[8] T. Ling, L. Xie, J. Zhu, H.M. Yu, H.Q. Ye, R. Yu, Z. Cheng, L. Liu, G.W. Yang, Z.D. Cheng, Y.J. Wang, X.L. Ma, Nano Letters 9 (2009) 1572–1576.
[9] R.M. Wang, O. Dmitrieva, M. Farle, G. Dumpich, H.Q. Ye, H. Poppa, R. Kilaas, C. Kisielowski, Physical Review Letters 100 (2008) 017205.
[10] V.Y. Shevchenko, A.E. Madison, A.L. Mackay, Acta Crystallographica A 63 (2007) 172–174.
[11] H.W. Kroto, K. Mckay, Nature 331 (1988) 328–331.
[12] L. Zeger, E. Kaxiras, Physical Review Letters 70 (1993) 2920–2923.
[13] W. Man, M. Megens, P.J. Steinhardt, P.M. Chaikin, Nature 436 (2005) 993–996.
[14] S. Matsumoto, Y. Matsui, Journal of Materials Science 18 (1983) 1785–1793.
[15] J. Buhler, Y. Prior, Journal of Crystal Growth 209 (2000) 779–788.
[16] R.C. Mani, M.K. Sunkara, Diamond & Related Materials 12 (2003) 324–329.
[17] H. Sawada, H. Ichinose, Diamond & Related Materials 14 (2005) 109–112.
[18] A. Haji-Akbari, M. Engel, A.S. Keys, X. Zheng, R.G. Petschek, P. Palffy-Muhoray, S.C. Glotzer, Nature 462 (2009) 773–778.
[19] S. Delclos, D. Dorignac, F. Phillipp, F. Silva, A. Gicquel, Diamond & Related Materials 9 (2000) 346–350.
[20] D. Shechtman, Journal of Materials Science 41 (2006) 7720–7724.
[21] Z. Yu, U. Karlsson, A. Flodstrom, Thin Solid Films 342 (1999) 74–82.
[22] Q. Wei, M.N.R. Ashfold, Y.A. Mankelevich, Z.M. Yu, P.Z. Liu, L. Ma, Diamond & Related Materials 20 (2011) 641–650.
[23] Q.-p. Wei, Z.M. Yu, M.N.R. Ashfold, J. Ye, L. Ma, Applied Surface Science 256 (2010) 4357–4364.
[24] R. Polini, G. Mattei, R. Valle, F. Casadei, Thin Solid Films 515 (2006) 1011–1016.
[25] Q.P. Wei, Z.M. Yu, L. Ma, D.F. Yin, J. Ye, Applied Surface Science 256 (2009) 1322–1328.
[26] N.G. Shang, C.H. Lee, X.T. Zhou, F.Y. Meng, C.Y. Chan, S.T. Lee, I. Bello, Journal of Vacuum Science and Technology A: Vacuum Surface Films 19 (2001) 2968–2973.
[27] Y.S. Li, A. Hirose, Chemical Physics Letters 433 (2006) 150–153.
[28] E. Nakamura, K.K. Hirakuri, M. Ohyama, G. Friedbacher, N. Mutsukura, Journal of Applied Physics 92 (2002) 3393–3396.
[29] M. Gowri, W.J.P. van Enckevort, J.J. Schermer, J.P. Celis, J.J. ter Meulen, J.G. Buijnsters, Diamond & Related Materials 18 (2009) 1450–1458.
[30] N. Kohmura, K. Sudoh, K. Sato, K.K. Hirakuri, K. Miyake, G. Friedbacher, Diamond & Related Materials 14 (2005) 283–287.
[31] J.G. Buijnsters, P. Shankar, J.J. Ter Meulen, Surface and Coatings Technology 201 (2007) 8955–8960.
[32] Q. Wei, Z.M. Yu, M.N.R. Ashfold, Z. Chen, L. Wang, L. Ma, Surface and Coatings Technology 205 (2010) 158–167.
[33] Q.-p. Wei, Z.M. Yu, M.N.R. Ashfold, L. Ma, Z. Chen, Diamond & Related Materials 19 (2010) 1144–1152.
[34] Q. Wei, M.N.R. Ashfold, Y.A. Mankelevich, Z.M. Yu, P.Z. Liu, L. Ma, Diamond & Related Materials 20 (2011) 641–650.
[35] Y.A. Mankelevich, A.T. Rakhimov, N.V. Suetin, Diamond & Related Materials 7 (1998) 1133–1137.
[36] Y.A. Mankelevich, N.V. Suetin, M.N.R. Ashfold, J.A. Smith, E. Cameron, Diamond & Related Materials 10 (2001) 364–369.
[37] J.E. Butler, Y.A. Mankelevich, A. Cheesman, J. Ma, M.N.R. Ashfold, Journal of Physics: Condensed Matter 21 (2009) 364201.
[38] V.F. Neto, R. Vaz, N. Ali, M.S.A. Oliveira, J. Gracio, Diamond & Related Materials 17 (2008) 1424–1428.
[39] A. Bohner, R. Janisch, A. Hartmaier, Scripta Materialia 60 (2009) 504–507.